

# Optimization of high-performance field emission rare earth tungsten alloy cathodes\*

Tao Wu,<sup>1,2</sup> Jinxing Zheng,<sup>2,†</sup> Haiyang Liu,<sup>2</sup> Yudong Lu,<sup>2</sup> Yifan Du,<sup>1,2</sup> Meiqi Wu,<sup>1,2</sup> Jiaming Shi,<sup>2</sup> and Maolin Ke<sup>1,2</sup>

<sup>1</sup>University of Science and Technology of China, Hefei, 230026, China

<sup>2</sup>Institute of Plasma Physics, Hefei Institutes of Physical Science, Chinese Academy of Sciences, Hefei 230031, China

The cathodes, as the electronic emission source of all kinds of electronic vacuum devices and spacecraft potential control system, its performance not only affects the overall efficiency of the equipment, but also limits the most important factors of the system long life and high reliability. In the field of space propulsion, the principle of electron emission from conventional cathodes mainly consists of thermal emission and field emission. Therefore, based on first-principles calculations using density functional theory, this study constructs atomic models of W cathode surfaces doped with different rare earth atoms. Using a  $(2 \times 2 \times 1)$  W (001) surface model, 1 ML of O atoms is absorbed on the top site of the surface, followed by doping rare earth atoms (La, Ce, Y) into the vacancy sites of the W-O lattice. The work functions of the system with rare earth atom coverages of 0.5 ML and 1 ML were calculated. Through liquid phase synthesis, plasma discharge sintering, and heat treatment, nano-scale second phase rare earth oxides ( $\text{La}_2\text{O}_3$ ,  $\text{CeO}_2$ ,  $\text{Y}_2\text{O}_3$ , etc.)-tungsten cathodes were produced. Different ignition experiments were designed to simulate various operating conditions. The cascade arc plasma source was used for mass-loss and lifetime prediction tests on the cathode materials. After testing, Scanning Electron Microscopy and Energy Dispersive Spectrum microscopic characterizations of the cathode materials were conducted to analyze their composition, morphology, and elemental distribution. Optimization results reveal that the W-La, W-Ce, and W-Y cathodes prepared with this method exhibit excellent ablation resistance and plasma bombardment endurance at high temperatures. The nanoscale dispersion of the doped phases endows the cathode with superior electron emission properties, enhancing the overall efficiency of the system. Under plasma density of  $1.0 \times 10^{19} \text{ m}^{-3}$  and working temperature of 2000 K, the projected lifetime of rare earth tungsten alloy cathodes exceeds 2000 hours.

Keywords: Field emission cathode, Rare earth tungsten alloy, First-principles, calculations, Work function.

## I. INTRODUCTION

As the primary and neutralizing electron source of various electronic vacuum devices and spacecraft potential control systems, the performance of the cathodes not only affects the overall efficiency of the system, but is also the most important factor limiting long service life and high reliability of the system [1, 2]. In the 1960s, cathodes were first applied to electric propulsion at the Lewis Research Centre and Houston Research Laboratory in the U.S.A. After decades of development, cathode technology has been greatly developed, including characterisation of cathode working plume modes, sputtering corrosion properties of cathode components, emitter working mechanisms, and validation of cathode working life [3–7].

Compared with various conventional thermal cathodes, field emission cathodes have a series of advantages, such as fast startup, room temperature operation, no preheating delay, and high current density, which has been applied in many fields such as electron beam lithography, vacuum diodes and space propulsion systems, and other fields [8]. At present, in the field of vacuum devices, the commonly used cathode materials are Ba-W cathodes, lanthanum hexaboride ( $\text{LaB}_6$ ) and dodecalcium heptaaluminate ( $\text{C12 A7}$ ) cathode materials, as well as new cathode materials developed on the basis of this,

and the advantages of the application of different emitter materials are different [9–12]. The Ba-W cathode consists of a mixture of sintered porous tungsten impregnated with barium oxide, calcium oxide, and alumina, where porous tungsten is the substrate and the mixture is the raw material. the Ba-W cathode has an escape power of about 2.1 eV and an operating temperature of about 1300 K, but it has high requirements for the working medium. the  $\text{LaB}_6$  is generally formed by the mechanical processing of powder pressurised and sintered polycrystalline structured rods, and has an escape power of about 2.7 eV, the working temperature exceeds 1800 K, and the long time high temperature service makes its power consumption larger. In recent years, theories have shown that C12 A7 compounds have lower escape power (theoretically 0.6 eV) and operating temperature (theoretically 900 K), and although no conclusion has been drawn from experiments, their excellent performance has attracted a great deal of attention from domestic and foreign researchers. Future cathode research will also focus on the electron escape work of the cathode emitter and the cathode operating temperature [13, 14]. However, in the Magneto Plasma Dynamic Thruster (MPDT), the cathode, as a core component, is in the center of the high-energy plasma plume, with an instantaneous ignition voltage of up to several thousand volts, an operating temperature higher than 1500 K, and an extremely harsh working environment, which puts forward high requirements for the cathode material and structure [15].

Metallic materials are the earliest researched and most widely used field emission materials, mainly W, Mo, Ta, etc. However, pure W has high electron escape power and is prone to difficult arc initiation and breakdown at low voltage. However, pure W has a high electron escape power, which makes

\* Supported by the Key project of National Natural Science Foundation, Grant No.52437001, The Key Research Program of Chinese Academy of Sciences, Grant No. KGFZD-145-23-53, and The HFIPS Director's Fund, Grant No. YZJJ2022 03-CX.)

† Corresponding author, jxzheng@ipp.ac.cn

it easy to appear phenomena such as difficult to start an arc and difficult to break down at low voltage. In addition, due to La, Ce, Y and other rare earth elements have lower escape power and higher melting point, it has been shown that the addition of rare earth oxides with lower escape power to W can significantly improve the ablation resistance of the cathode. In recent years, North American researchers and scholars have prepared E3 ternary electrodes with  $\text{ZrO}_2$  as an additive, and the main components are  $\text{W-La}_2\text{O}_3\text{-Y}_2\text{O}_3\text{-ZrO}_2$ . Zhu Wenguang et al. compared the arc initiation performance of E3 electrodes with that of traditional multielement electrodes, and in the ablation at a current of 200 A for 5 h, E3 electrodes showed the smallest amount of loss by ablation, and the dimensional stability was good, and the degree of recrystallisation was weak. Therefore, based on the traditional cathode electron emission theory and traditional cathode material types this study will use the high melting point component W as the cathode substrate, doped with different types and contents of rare earth elements, and complete its various performance tests and ground prototype experiments to verify [16–18].

Atomic models were constructed with tungsten(W)-O surfaces doped with various rare earth atoms (La, Ce, Y), using first-principles calculations and density functional theory(DFT). Calculations for the work functions were conducted for the models of 0.5 ML and 1.0 ML doping levels. The results showed that doping rare earth elements greatly lowered the work function of the alloy cathode, improving electron emission performance, and that 0.5 ML doping in W-O lattice sites resulted in the lowest work function.

In the present study, nano-doped rare earth tungsten cathode materials were prepared using liquid-phase synthesis and plasma discharge sintering techniques. A series of ignition tests on the thruster prototypes were conducted along with microstructural characterization experiments. Electron emission performance, ignition performance, and efficiency of a tungsten alloy cathode doped with various elements and proportions were tested.

In addition, based on the working principle of cathode for various vacuum devices, in view of the existing experimental conditions, the long-life test of the whole machine is subject to greater constraints. Therefore, this study independently conducts a life assessment experiment for cathode, and conducts a mass-loss-life prediction of cathode through a self-developed cascade arc plasma generator source. The results show that the nano rare-earth tungsten alloy cathode has better electron emission performance than the conventional cathode, in which the lanthanum oxide doped tungsten alloy with different mass fractions makes the cathode material escape work reduced significantly; after the independent life test of the cathode, the preliminary prediction of the rare-earth tungsten alloy cathode life reaches 2000 h.

## II. ELECTRON EMISSION PRINCIPLE OF FIELD EMISSION CATHODE

The emission of cathodes used in thruster systems primarily relies on the principles of thermionic emission and field emission [19]. Thermionic emission follows the Richardson equation:

$$j_0 = [AT_K^2] \exp(-\phi_k/kT_K) \quad (1)$$

As shown in Equation(1),  $j_0$  represents the zero-field emission current density.  $A$  is the theoretical value of the material's emission constant,  $T_K$  is the cathode operating temperature, and  $\phi_k$  represents the material's work function [20].

Similar to the theoretical derivation of the thermionic emission equation, Fowler and Nordheim developed the field emission theory for metals. They assumed the following: (1) the distribution of band electrons conforms to the Fermi-Dirac distribution; (2) a smooth, planar metal surface is considered, ignoring atomic-scale irregularities; (3) classical image forces affecting electrons are taken into account; (4) the work function distribution is uniform. Under these assumptions, the following equation holds:

$$j_0 = \frac{1.54 \times 10^{-6} \xi^2}{\phi_k} \exp \left[ -\frac{6.83 \times 10^7 \phi_k^{3/2}}{\xi} \theta(y_0) \right] \quad (2)$$

In Equation(2),  $\xi$  represents the electric field strength, measured in V/cm. Where  $\theta(y_0)$  is a slow-variable function of  $\xi$ ,

$$y_0 = \left( 3.79 \times 10^{-4} \frac{\sqrt{\xi}}{\phi_k} \right) \quad (3)$$

According to the electron emission equations above, the zero-field emission current density  $j_0$  is closely related to parameters such as the material's work function, temperature, and electric field strength. Theoretically, the lower the work function of the cathode material, the more readily electrons within the material can overcome the surface potential barrier to emit from the cathode surface. Additionally, the operating temperature  $T_K$  and electric field strength  $\xi$  are directly proportional to the zero-field emission current density  $j_0$  of the cathode. At lower temperatures, thermionically emitted electrons that overcome the barrier contribute negligibly to the emission current, with the emission primarily consisting of field-emitted electrons near the Fermi level [21].

For the work function of cathode materials, the periodic arrangement of lattice ions is interrupted at the metal-vacuum boundary, thereby disrupting the periodicity of the potential field [22]. The potential energy increases in a specific manner and approaches zero at infinity, forming the surface potential barrier of the metal. When electrons move to the metal surface and attempt to escape, they are hindered by this surface barrier, which is defined as the material's work function.

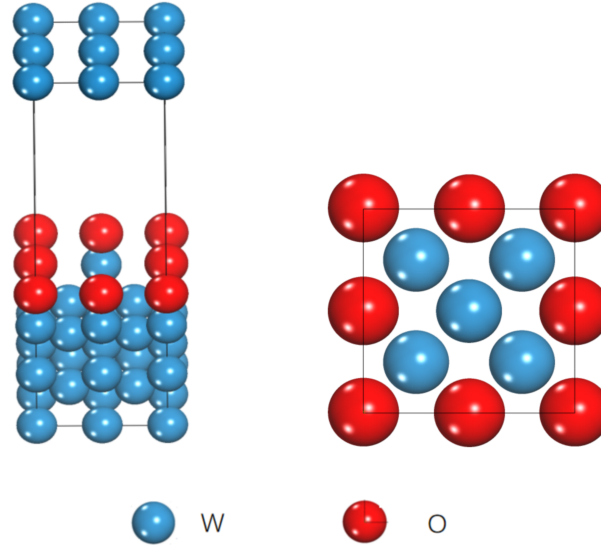


Fig. 1. Top-Site Adsorption of O Atoms on W(001) Surface.

$$\phi_k = E_V - E_F \quad (4)$$

All electrons attempting to escape from the metal must have energy at least equal to the Fermi level plus the value of the work function and follow a statistical distribution. Their average energy equals 32 KT, with each degree of freedom contributing an average energy of 12 KT, consistent with the results of kinetic molecular theory [23].

On the other hand, the cathode evaporation rate increases sharply with rising cathode operating temperature. Cathode evaporation directly impacts the cathode's lifespan, grid emission, and inter-electrode insulation performance. Ideally, a cathode should have high emission capability, requiring a low work function and minimal evaporation. Considering these two requirements, a quality factor  $F$  can be used to represent the performance:

$$F = \phi_k \times 10^3 / T_e (eV/K) \quad (5)$$

$T_e$  is the temperature (K) at which the material's vapor pressure reaches  $10^{-5}$  mmHg. To ensure thruster performance, the cathode temperature should not exceed its "vapor pressure temperature"  $T_e$  [24].

Therefore, the selection and optimization of cathode emitter materials need to balance electronic emission performance with thermodynamic properties. Higher electron emission performance can enhance cathode discharge efficiency and overall thruster efficiency, while better thermodynamic properties extend the service life of the cathode under extreme operating conditions. The research in this paper will mainly start from the simulation and experimental optimisation of cathode material components to reduce the emitter escape work, and verify the key parameters of cathode material such as electron

emission performance, lifetime, and ablation performance, so as to further complete the research on the cathode for high-performance field-emission space propulsion.

On the basis of traditional field emission cathode research, new field emission cathode has become a current research hotspot. Researchers at the National University of Defense Technology prepared a carbon fiber composite graphite cathode and tested its electron emission performance, which showed that the field emission threshold electric field of the 40% (mass fraction) carbon fiber composite graphite cathode was reduced from 143 kV/cm to 119 kV/cm, a reduction of about 16.8%, and due to the characteristics of the structural stability of the carbon fibers in the process of electron emission, the carbon fibers conformity is also favours the improvement of cathode service life [25]. Maksim A Chumak et al, Ioffe Research Institute, St. Petersburg, Russia, used atomic layer deposition (ALD) to produce field-emission cathodes with carbon nanotube (CNT) arrays coated with ultrathin nickel oxide (CNT/NiO), and proposed for the first time to reduce the figure of merit of the field-emission nanocomposite CNT/NiO cathode by changing the chemical composition of the oxide coatings, and it was demonstrated that, according to the secondary electron cut-off energy, the work function of pure CNTs is 4.95 eV, and the work function of NiO layer deposited on CNTs after heat treatment is reduced [26].

### III. FIRST-PRINCIPLES STUDY ON THE SURFACE WORK FUNCTION OF RARE EARTH TUNGSTEN ALLOY CATHODE

Quantum mechanics is an important foundation of modern physics and one of the greatest discoveries of the 20th century. Using quantum mechanics, it is possible to explain and predict the physicochemical properties of a wide range of sys-

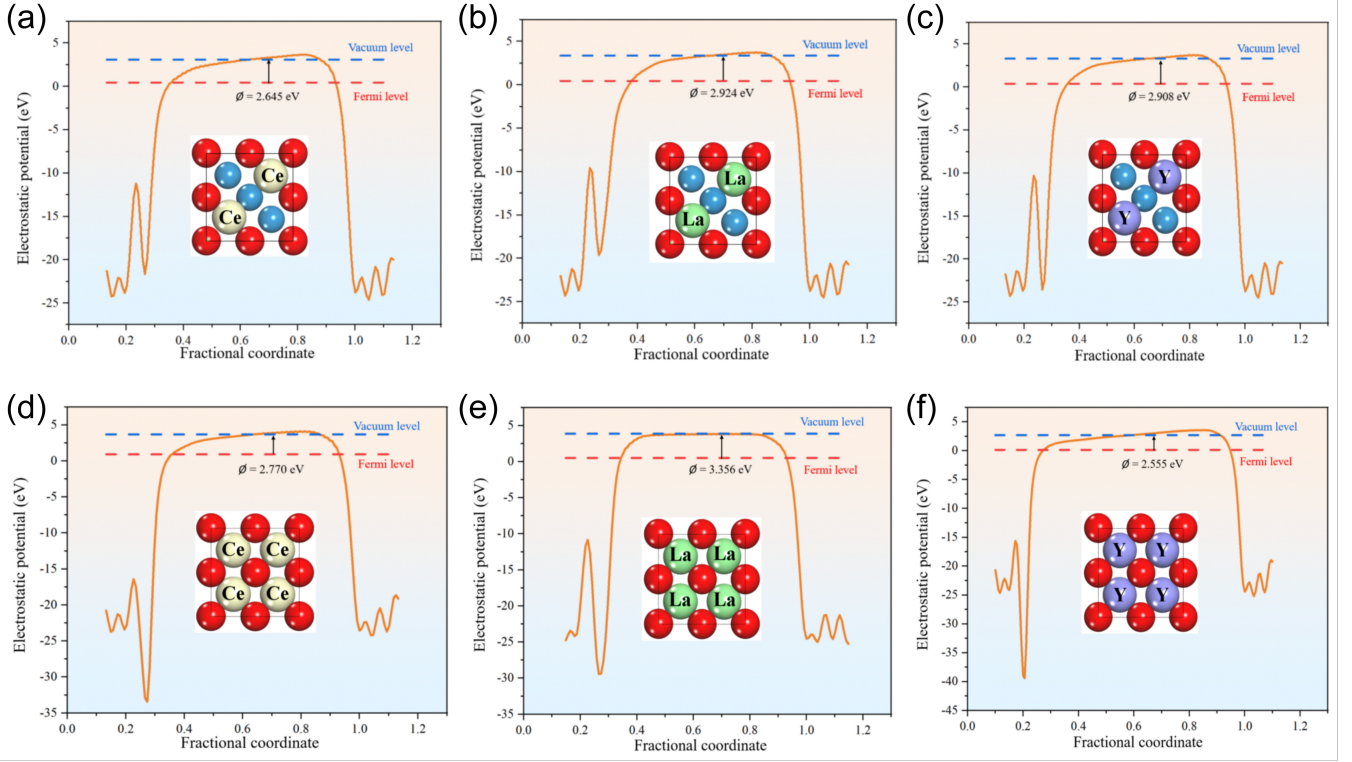


Fig. 2. W-O Crystal Surface Doped with rare earth atoms model and work function calculation.(a) Doped with 0.5 ML Ce; (b) Doped with 0.5 ML La; (c) Doped with 0.5 ML ML Y; (d) Doped with 1.0 ML Ce; (e) Doped with 1.0 ML La; (f) Doped with 1.0 ML Y.

tems and to quantitatively analyze the laws of their electronic motion. The first principle is a computational method based on quantum mechanics to study the properties of materials from the point of view of electron motion. The wave function contains all the information of the computational system, which greatly limits the scope of its practical applications, and the establishment of the density functional theory solves the problem of the complexity of the wave function. The basic idea of density functional theory is to change the characteristics based on the orbital wave function, with the particle density function to express the system base state of each physical quantity, to the electron density function represents the system energy [27, 28].

Material Studio material simulation software incorporates a variety of three-dimensional scale simulation calculation methods, which can complete the cross-scale scientific research from the microscopic electronic structure to the macroscopic performance prediction [29]. It is on the basis of this advantage that the atomic-scale emission structure was modeled with the use of the Materials Studio in the current work. Geometric optimization was made for tungsten alloy models doped with various rare earth elements. Further on, the relaxation of surface atoms was conducted and work function was calculated under convergence conditions. The pseudopotential method was realized for solution of Schrödinger equation, while computations of work function were performed in LDA functional and PBE-GGA functional. The work function of the (001) crystal plane for tungsten is calculated in

order to assess the possible effect the doped elements have on the current density of the cathode emission [30].

The models mainly include the following: the adsorption of O atoms and La atoms on a tungsten surface, adsorption of O atoms and Ce atoms on a tungsten surface, and adsorption of O atoms and Y atoms on a tungsten surface.

The current work has used the CASTEP density functional calculation module of Materials Studio, which is based on a plane-wave basis set. Among the well-known classical algorithms in CASTEP, the main one is the plane-wave pseudopotential method. By moving the model of a tungsten atomic structure and geometric optimization, it was possible to find the ground state with the lowest energy. We used the default number of maximum steps, while the cutoff energy was 278.0 eV. The method of calculation was "Fine" and for the rest of the parameters that were given, we kept them the same as the default. Under the ultrasoft pseudopotential, GGA was being applied, and the functional from Perdew-Burke-Ernzerhof was picked to describe the electron exchange-correlated interactions [31].

O atomic layer was adsorbed on the surface of the supercell  $W(2 \times 2 \times 1)$ . According to the related computational literature, the larger the adsorption energy is, the more stable the adsorption system is. In fact, the adsorption energies of O atoms on the top site, bridge site, and hollow site of W supercell are about 9.11 eV, 7.40 eV, and 8.20 eV, respectively; this means the O atoms are preferentially adsorbed on the top site shown in Figure 1 [32].



On the W-O (top-site) surface, rare earth atoms with varying coverages were adsorbed. Similar to O atoms, rare earth atoms on the  $(2 \times 2 \times 1)$  W(001)-O (top-site) surface also have three possible adsorption positions. Due to the larger atomic radius of rare earth elements, adsorption at the top and bridge sites causes significant lattice distortion in the W lattice. Computational results indicate that rare earth atoms are more likely to adsorb at hollow sites on the W-O (top-site) surface. The formula for calculating the adsorption energy of rare earth atoms is as follows:

$$E_{ad} = -\frac{1}{N}(E_{La+W(001)-O(top)} - NE_{La} - E_{W(001)-O(top)}) \quad (6)$$

As shown in Figure 2a to 2c, the work function for rare earth atoms in the W-O crystal with a coverage of 0.5 ML was calculated using Equation (6). Because rare earth atoms readily lose their two outermost valence electrons, transferring them to the inner O atoms, the electron density of the coverage layer is lower than that of the substrate surface layer. This results in a dipole layer with a positive charge on the outside, raising the surface potential and reducing the barrier height.

Similarly, this study further calculated the work function of W-O crystals with a rare earth atom coverage of 1.0 ML, meaning that rare earth atoms fully occupy the hollow sites in the W crystal, as shown in Figure 2d to 2f.

Table 1. Work Function of W-O (Top-Site) Doped with Different Rare Earth Atoms.

W(001)-O Top-Site Doping	Work Function (eV)
0.5 ML Ce atoms	2.645
0.5 ML La atoms	2.924
0.5 ML Y atoms	2.908
1.0 ML Ce atoms	2.770
1.0 ML La atoms	3.356
1.0 ML Y atoms	2.555

As marked in Table 1, the calculational results of work function for W-O (top-site) doped with 0.5 ML and 1.0 ML of different rare earth atoms show that the large atomic radius of rare earth elements results in large lattice distortion when fully occupying the hollow sites in the W crystal, and therefore such a system is unstable. When the number of adsorbed atoms increases above each optimal coverage, the interactions between dipoles increase gradually. Here, the middle atoms are depolarized by an electric field of adjacent dipoles. The reduction of a dipole moment increases the work function.

Comparing the data in the table, doping rare earth atoms into the W crystal reduces the surface work function in all cases, validating the feasibility of this study's approach to optimize cathode electron emission performance by doping tungsten with rare earth elements, thereby enhancing the efficiency of magnetoplasma thrusters. Additionally, the calculation results show that doping 0.5 ML La or Ce atoms at the W-O (top-site) achieves the greatest reduction in work function. Due to the relatively smaller radius of Y atoms, full Y atom doping into the hollow sites of the tungsten crystal

results in minimal lattice distortion, and its work function is slightly reduced compared to 0.5 ML Y doping.

#### IV. EXPERIMENTAL STUDY ON CATHODE OF RARE EARTH TUNGSTEN ALLOY

##### A. Synthesis and processing of rare earth tungsten alloy cathodes

For various vacuum electronics and space propulsion systems, the primary requirements for cathodes are superior electron emission capability and high ablation resistance to withstand impacts from high-energy particles. Experimental research indicates that the electron emission performance, melting point, and ablation resistance of rare earth tungsten alloy cathodes are closely related to the chemical properties, physical dispersion, and percentage content of the nano-doped phase. We synthesized W-La<sub>2</sub>O<sub>3</sub> alloy cathodes with different doping levels and studied their electron emission performance at various temperatures and voltages for different W-La<sub>2</sub>O<sub>3</sub> doping concentrations [33].

Figure 3a shows the flow process for the preparation of nano rare earth tungsten alloy cathode. In this study, the nano rare-earth tungsten alloy cathode raw material mixed powders were produced by two methods, namely, liquid-phase synthesis reduction method and ball milling method, and moulded with reference to the processing method of LaB<sub>6</sub> cathode emitter. The liquid-phase synthesis method is to mix tungstate, lanthanate and complexing reagent in deionised water according to the measured ratios, and then react for about 8 hours at the appropriate temperature, and then spray-drying is carried out to obtain the homogeneous raw material powders; the ball milling method is to use the planetary ball mill to mill the mixed powders for 4 hours at 240 rpm under argon gas at room temperature, with a ball-to-powder weight ratio of 8:1. After mixing the raw material powders, the powders were pressed into rods with a diameter of 16 mm by cold isostatic pressing at a pressure of 150 MPa, and then sintered at 2600 K for 4 h in a dry hydrogen atmosphere. Finally, in order to remove the oxide layer from the samples and to obtain a smooth surface, we ground the rods to a diameter of 9.0 mm using a computer numerical control (CNC) machine. The densities of the W-La samples were obtained using the Archimedes method, and the theoretical densities were calculated based on the fraction of each component as a function of the density, and the densities of the W-La cathodes obtained by the preparations in the present study were in the range of 98.5% - 99.5%. Figure 3b is the physical diagram of the W-La cathode prepared according to the above process [34–36].

After the cathode was processed, we measured its actual density using the Archimedes drainage method and compared it with its theoretical density to obtain the homogeneity parameters, as shown in Table 2. The densities higher than 98% proved that the sintered state of the cathode obtained by this method is dense and uniform, and the subsequent tests and experiments can be completed.

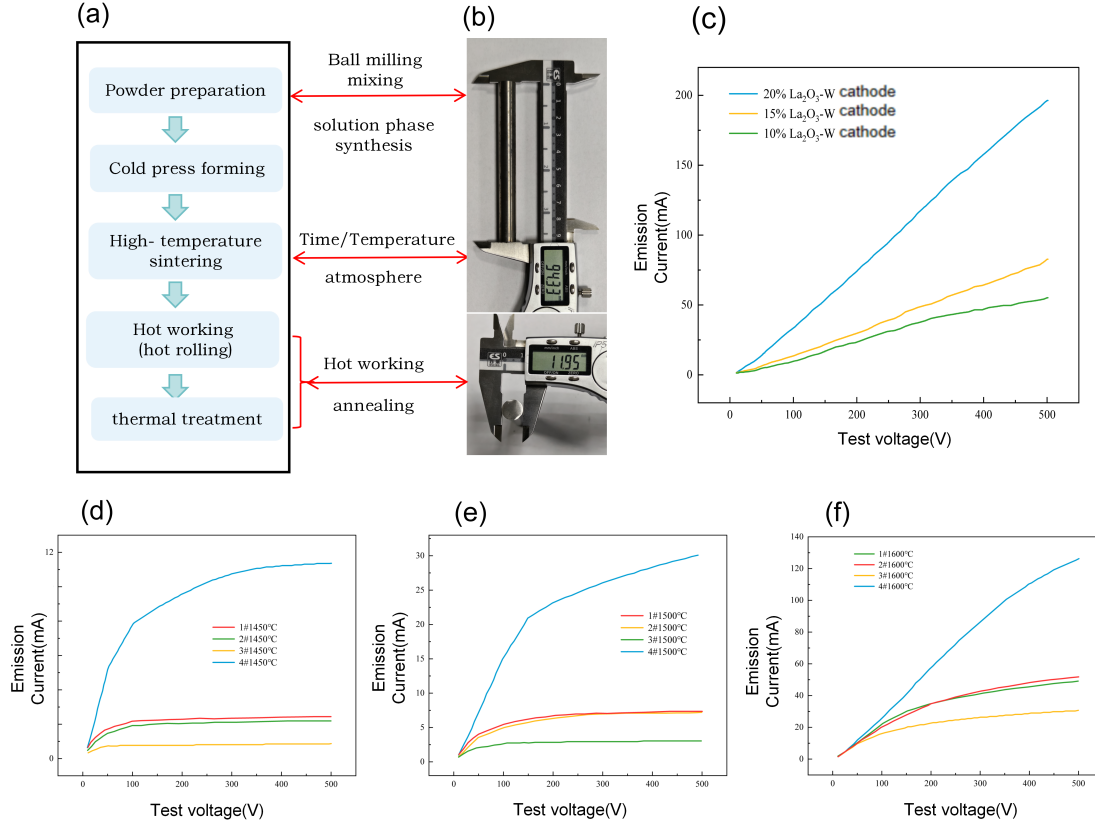


Fig. 3. (a)Processing workflow of rare earth tungsten alloy cathodes.(b)Physical drawing of cathode.(c)Electron emission properties of lanthanum oxide-doped tungsten cathodes with different contents.(d)-(f)Electron emission properties of different types of rare-earth cathodes and tungsten cathodes at 1450 °C,1500 °C and 1600 °C, respectively.1#:W-Zr-Y cathode;2#:W-Y cathode;3#:pure W cathode;4#:W-La15 cathode

The series of rare earth tungsten alloy cathodes we designed and processed are aimed at the extreme working environment of vacuum equipments and space thrusters. By optimizing the emitter composition, we aim to balance high electron emission performance with ablation resistance for extended service life. Figure 3c shows electron emission performance data for W cathodes doped with various mass fractions of W-La<sub>2</sub>O<sub>3</sub>. As W-La<sub>2</sub>O<sub>3</sub> content increases, the overall electron emission performance of the cathode improves significantly, confirming that adding low work function components to optimize emitter performance is feasible. In addition, we tested the electron emission properties of different doping types of cathodes at 1450 °C, 1500 °C and 1600 °C, respectively, as shown in Figures 3d to 3f. The results show that the emission current densities of the four cathodes tested in the experiments increase to different degrees with the increase of the test voltage and the test temperature, among which the W-La15 cathode has the largest increase; the pure W cathode no longer increases in the emission current density when the test voltage reaches the threshold value due to its lower electron emission current density of the pure W cathode no longer increases when the test voltage reaches the threshold value due

to its lower electron escape work.

In addition, we prepared W-Ce and W-Y rare earth tungsten alloy cathodes with different doping ratios using the same processing method and made preliminary predictions of their properties [37, 38]. During the sintering process of W-Ce cathode, due to the volatilisation of CeO<sub>2</sub>, which affects the stability of the hollow cathode discharge, the process needs to be strictly controlled, and it needs to be prepared by insulated sintering [39].

Table 2. Actual density and homogeneity of different types of cathodes.

Type of cathode	D <sub>A</sub> (g/cm <sup>3</sup> )	D <sub>T</sub> (g/cm <sup>3</sup> )	Homogeneity (%)
W-Y10 cathode	18.69	18.81	99.4±0.1
W-La10 cathode	18.87	18.98	99.4±0.1
W-La15 cathode	18.65	18.79	99.3±0.1
W-La20 cathode	18.46	18.62	99.1±0.1

## B. Independent service life experiment using cascade arc plasma source

Under conditions of existing experimental possibilities, the verification of the service life of cathodes is a long-time and expensive process, and even more expensive are tests of life validation conducted together with thrusters. As space missions have imposed longer lives on electric propulsion systems, full-life ground testing has become increasingly impractical. For instance, the ground-tested ion thruster for NASA's \*Deep Space 1\* mission lasted for 30 352 hours, which is more than five years [40]. In comparison, the JIMO mission would have used six ion thrusters powered by nuclear energy as its main propulsion; these would have to individually be rated for 83,000-hour lives. Assuming an efficient test duration of 75 percent, a 1.5-times redundancy life test would take approximately 19 years [41]. **The extended life test of the U.S. NEXT ion thruster for the subsequent deep space exploration mission started in 2005, and a total of 51 184 h life tests were conducted until 2017, consuming 918 kg of xenon gas. Therefore, under the existing experimental conditions, we will carry out a rapid life test method to evaluate the cathode life in combination with relevant experimental parameters, which also greatly reduces the life test time and cost [42].**

We have developed a cascade arc plasma source to simulate the real working environment of rare earth tungsten alloy cathodes. This consists of a vacuum system, the power supply system, the superconducting magnet system, the plasma generation device, the gas supply system, the water cooling system, and the Langmuir probe system, as shown in Figure 4a.

In this paper, it is considered that the tip morphology of the cathode changes significantly when the mass loss of the cathode reaches 10% - 15%. This reduces the effectiveness of small-hole current limitation and leads to inability to maintain stable discharge when the propellant flow rate exceeds the set operating range, and the cumulative operating time under rated conditions cannot be achieved. Beyond this point, the cathode is to be considered functionally degraded and at the end of its service life.

Therefore, as shown in Figure 4c to 4e, we used our custom cascade arc plasma source to simulate the thruster's experimental environment by placing the cathode within the plasma source and setting specific plasma density and temperature parameters. Material ablation and service life predictions were conducted based on mass loss over a specified experimental duration. This study performed independent lifetime experiments and comparisons for W-La cathodes, W-Ce cathodes, and pure W cathodes [43].

The mass loss of the three experimental cathode materials under the conditions of 3 h experimental duration with the plasma density up to  $1.0 \times 10^{19} \text{ m}^{-3}$  measured by Langmuir probe and the temperature up to 1300°C measured by the bottom plate temperature probe is shown in Figure 4b. Based on parameters such as gas flow rate, input current, magnetic field strength, and plasma density, the service life of the W-La cathode is estimated at approximately 3000 hours, and for the W-Ce cathode, about 1100 hours. This reduction is at-

tributed to decreased thermal resistance of the cathode matrix as rare earth element content increases, leading to higher mass loss under extreme operating conditions and consequently reduced service life.

Thus, in optimizing the performance of cathodes, it is essential to ensure both excellent electron emission performance and high ablation resistance.

## C. Microstructural characterization of rare earth tungsten alloy cathodes

The melting, sputtering, and eventual deposition on the surface of the cathode material due to the W matrix are critical factors affecting the lifespan and efficiency of the cathode material. Preliminary analysis of the deposits shows no new elements, consisting solely of tungsten oxides, which exhibit valence changes at high temperatures [44].

**The rare earth tungsten alloy cathode we prepared was severely ablated after a long ignition experiment. The cathode surface was characterised and analyzed by SEM before and after the experiment, as shown in Figure 5. Among them, Figures 5 a to 5 c show the morphological characterisation analysis of W-La15 cathode before ignition experiment, the  $\text{La}_2\text{O}_3$  particles are uniformly distributed on the smooth W substrate, and the elemental content distribution is shown in Figures 6 a to 6 d. This indicates that the low fugitive work components in the rare earth tungsten alloy cathode prepared by our ball milling method and liquid phase synthesis method are uniformly dispersed, which provides a favourable condition for the improvement of the electron emission performance of the cathode. Figures 5 c to 5 e show the morphological characterisation of the cathode after the ignition experiments, and it can be clearly seen that the cathode tip hole shrinks severely due to the prolonged ignition and plasma sputtering during the working process, which also leads to a more difficult cathode ignition arc initiation under the same ignition power and propellant flow rate. This result suggests that, in order to obtain the same or greater propulsive efficiency, the ignition voltage needs to be increased in order to break through the cathode and complete the ignition, which also causes greater damage to the cathode ignition instant. As can be seen in the figure, the cathode surface is left with inhomogeneous holes from the depletion of  $\text{La}_2\text{O}_3$  particles, which indicates the feasibility of this study to improve the electron emission performance of the cathode through the addition of a low fugitive work component to the W matrix. Therefore, our study of the cathode needs to balance its ablation performance with the optimisation of the ignition conditions.**

**The W-La cathodes before and after the experiment were further analysed by energy spectrum as shown in Figure 6. Figures 6 a to 6 d show the atomic energy spectra and elemental analysis results of the W-La cathode before the experiment, in which the dark-coloured part is the area where the  $\text{La}_2\text{O}_3$  particles are located, which is highly overlapped with the results of the point-scan elemental analysis in this area, and the results of the face-scan elemental analysis indicate that the main material of the whole cathode material**

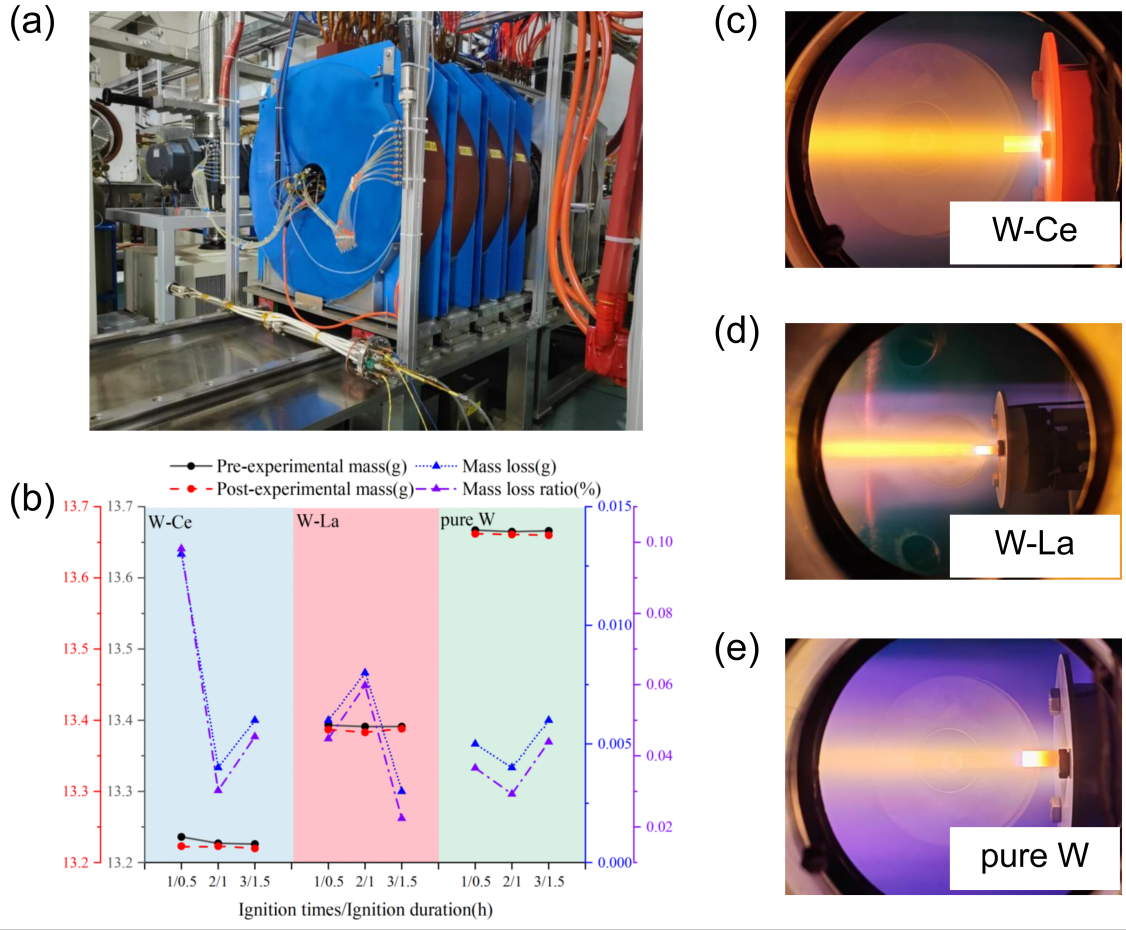


Fig. 4. Ablation life prediction experiment by cascade arc plasma generation source system. (a) Cascade arc plasma generation source system (Institute of Plasma Physics, Chinese Academy of Sciences, China); (b) Test cathodes mass loss data chart; (c) W-Ce cathode test; (d) W-La cathode test; (e) Pure W cathode test.

is tungsten, and the  $\text{La}_2\text{O}_3$  particles are uniformly dispersed on the surface of the W substrate. Figures 6 e to 6 h show the atomic energy spectra and elemental analysis results of the W-La cathode after the experiment. The surface-scanning elemental analysis results show that the content of W is as high as 65.7%, followed by O element, and the content of rare earth La is as low as 1.6%, which indicates that the La is doped into W matrix in the form of  $\text{W-La}_2\text{O}_3$ , which is consumed in the process of discharging to complete the electron emission. Analysis of the particulate matter on the cathode surface in Figure 6 g shows that it is an oxide of W. The melting and recrystallisation of the W matrix at high temperatures changes the valence state to form different W oxides.

The characterization results show that the rare earth oxide  $\text{W-La}_2\text{O}_3$ , due to its low work function, allows electrons near the Fermi level of La to overcome the surface barrier and emit from the material under high voltage between the cathode and anode. It results in the appearance of pores, which can be distributed on the surface of emitters in a very uneven manner, and it also demonstrates that the poor work function given by rare earth elements has been wildly added in order to improve the total performance and efficiency of emitters.

Moreover, the density, size, and evenness of such pores on the surface depend on many factors, including the size of the second phase particle, the doping mass fraction, and the raw material mixing methods.

## V. RESULTS AND DISCUSSION

The cathode is one of the crucial components of various electronic vacuum devices and space propulsion systems, and the electron emission performance and ablation resistance of cathode materials against high-energy particle impacts directly affect the overall efficiency, performance and life of the system and other key indicators [45]. Therefore, the future research on cathode needs to consider the doping elements affecting the electron escape work of cathode materials, thus affecting the electron emission performance of cathode, in addition, the ratio of doping elements and W matrix affects the melting point of the overall alloy, that is, it affects the sputtering resistance of cathode, etc.; in addition, the preparation method of cathode also greatly affects its performance, and the optimization of the cathode preparation process enables



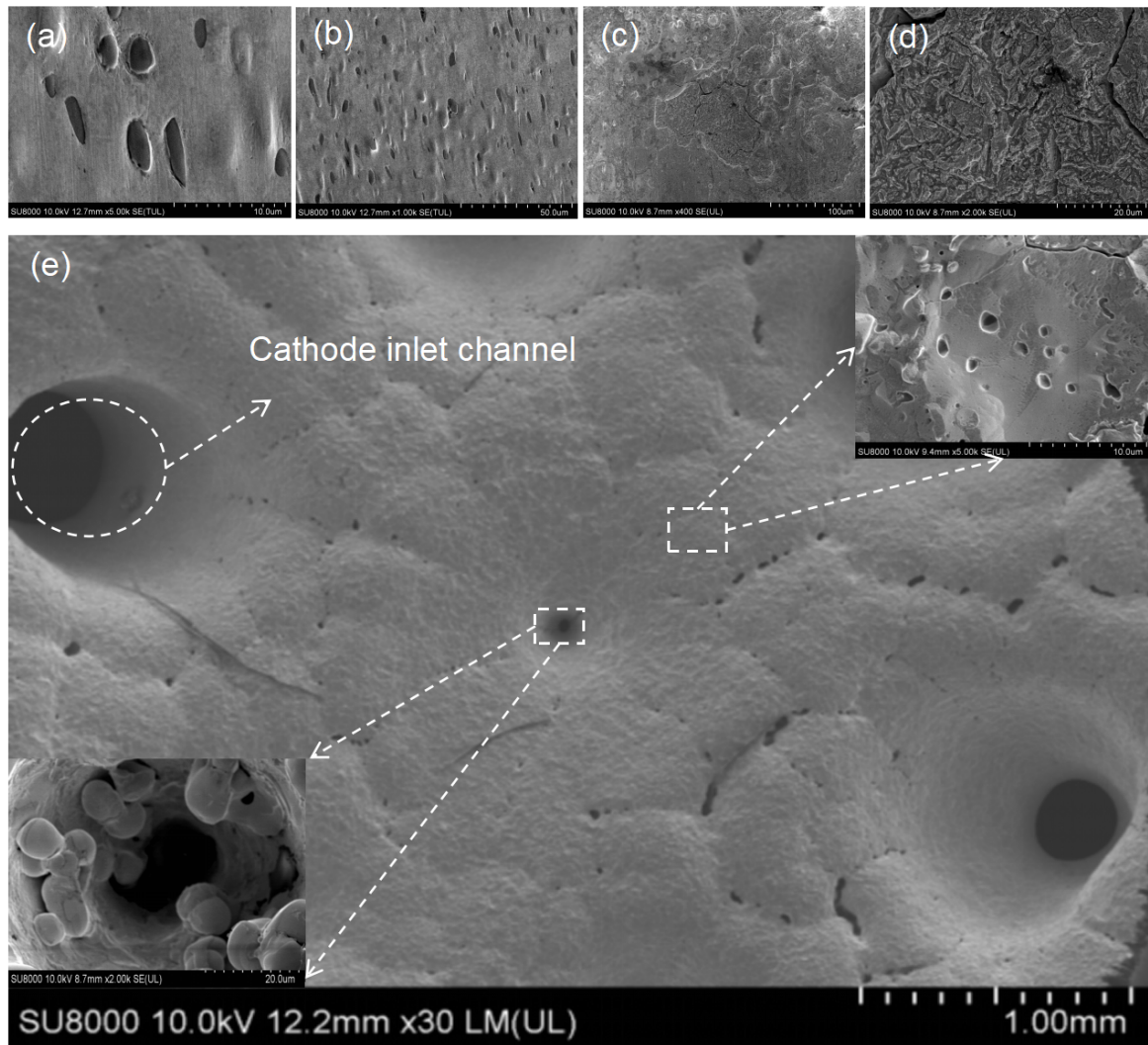


Fig. 5. Scanning Electron Microscopy (SEM) of W-La cathode before and after the experiment.(a)-(b) Scanning electron micrograph of W-La cathode before the experiment,5000 x and 1000 x, respectively; (c)-(d) Scanning electron micrograph of W-La cathode after the experiment,400 x and 2000 x, respectively; (e) Scanning electron micrograph of W-La cathode tip area after the experiment.

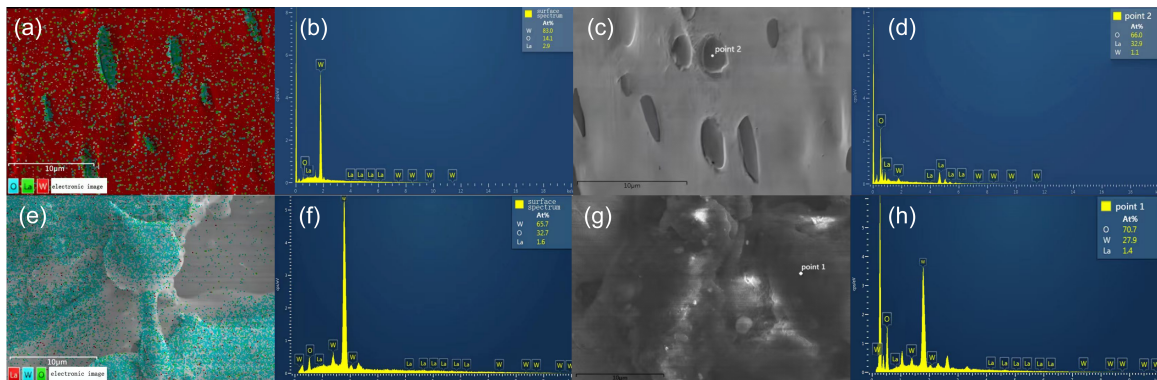


Fig. 6. Energy Dispersive Spectrum (EDS) of W-La cathode before and after the experiment.(a)-(d)Energy Dispersive Spectrum (EDS) of W-La cathode before the experiment,surface scanning and spot scanning,respectively; (e)-(h)Energy Dispersive Spectrum (EDS) of W-La cathode after the experiment,surface scanning and spot scanning,respectively.

the dopant phase to form a nano-sized in W matrix. dispersion, the better the dispersion, the better the improvement ef-

fect on the cathode emission performance.

In this paper, the optimization of high performance field emission rare earth tungsten alloy cathode is investigated by both simulation and experimental verification. Atomic models are built with Material Studio for rare earth elements adsorbed onto the W-O (top-site) surface; the relevant surface work functions are then calculated based on density functional theory. The work function values calculated were 2.645 eV, 2.924 eV, and 2.908 eV for 0.5 ML of Ce, La, and Y adsorbed on the W-O top site and 2.770 eV, 3.356 eV, and 2.555 eV for 1.0 ML of Ce, La, and Y, correspondingly. These results reflect that doping of rare earth atoms effectively reduces the surface potential barrier of the cathode, which confirms that doping of rare earth atoms is an effective method to enhance performances of electron emission for cathodes.

Some related studies have shown that the addition of 1%  $\text{La}_2\text{O}_3$  to W can improve its cutting performance and recrystallisation temperature, further optimising the WLa cathode sintering and processing. Of course, based on the Material Studio simulation result, in the paper, W-La, W-Ce, and W-Y cathodes with different treatment methods were prepared; a serial of ignition tests have been designed and performed; the results indicate that compared to pure tungsten cathodes, the operating condition for the rare earth tungsten alloy cathode operating is more stable with lower ignition voltage.

A cascade arc plasma source custom's development was also employed to simulate the real working environment that tungsten alloy cathodes face. On the basis of all the same quantity of these operational parameters, namely, the gas flow rate, input current, magnetic field strength, and plasma density, the service lives for the considered rare earth tungsten alloy cathodes were estimated. In terms of cathode theoretical life prediction research, the more mature research programmes are for Hall thrusters and low-power ion thrusters, with less research on the cathodes of high-power, high-ratio impulse magnetic plasma thrusters. The HET-80 Hall thruster underwent life verification tests at the Shanghai Institute of Space Propulsion (SISP) and the Beijing University of Aeronautics and Astronautics (BUAA), respectively. The full life test was carried out in the VF-6 vacuum chamber of the Shanghai Institute of Space Propulsion, with a cumulative working time of 9240 h; the 1:1 working life test was car-

ried out in the DT-2.5 vacuum chamber of the Space Plasma and Electric Propulsion Laboratory of the Beijing University of Aeronautics and Astronautics, with a cumulative working life of 8241 h [46]. Certainly, due to the more severe working environment of high-power magnetic plasma propellers and the higher working temperature, the cathode life will be greatly reduced. Therefore, factors such as cathode emitter material selection, ablation mechanism research and cathode processing technology will have an impact on cathode life, and the future cathode life optimisation research also needs to balance various factors, and the long-life high-performance cathode for magnetic plasma thruster will also be a research focus.

Optical microscopy, SEM, and EDS were conducted on the cathodes pre-experiment and post-experiment. The experimental results obtained show that the role of the rare earth doped in the tungsten alloy cathodes is to excite the outer valence electrons at high voltage and break down the propellant to form plasma. In continuous electron emission, the consumption of the rare earth atoms is gradual. However, with the increase of the doping ratio of rare earth, to a certain extent high-temperature resistance of the cathode declines and serious ablation occurs. Thus, by changing the ratio of doping atoms in the cathode, an optimization of the trade-off between excellent electron emission performance and good resistance against ablation can be achieved.

Based on the above research on different rare earth tungsten alloy cathodes, we believe that high-performance field emission rare earth tungsten alloy cathodes will have great application prospects in many aspects such as vacuum devices, space propulsion, etc., in which the excellent electron emission performance of tungsten-lanthanum cathode can greatly improve the emission efficiency of the cathode itself. The ablation mechanism of rare earth tungsten alloy cathode and the development of longer-life cathode will be the next research focus.

## VII. BIBLIOGRAPHY

- [1] D.R. Lev, I.G. Mikellides, D. Pedrini et al., Recent progress in research and development of hollow cathodes for electric propulsion. *Reviews of Modern Plasma Physics* **3**(1), 6 (2019). doi: 10.1007/s41614-019-0026-0
- [2] Y. Guo, Z. Nie, X. Xi et al., Advances in research on tungsten cathode materials. *J. Rare Earths* **29**(2), 200–205 (2005). doi: 10.13373/j.cnki.cjrm.2005.02.017
- [3] M. Mandell, I. Katz, *Theory of hollow cathode operation in spot and plume modes 30th AIAA (ASME/SAE/ASEE Joint Propulsion Conf. & Exhibit, 1994)*. doi:10.2514/6.1994-3134
- [4] I. Katz, M. Mandell, M. Patterson, M. Domonkos, *Sensitivity of hollow cathode performance to design and operating parameters*, in *35th Joint Propulsion Conference and Exhibit* (1999), p. 2576. doi:10.2514/6.1999-2576
- [5] M.T. Domonkos, A.D. Gallimore, M.J. Patterson, *An evaluation of hollow cathode scaling to very low power and flow rate*, in *Proceedings of the 25th International Electric Propulsion Conference* (IEPC Cleveland, Ohio, USA, 1997), pp. 97–189
- [6] J. Hendry, *Investigation of efficient designs of hollow cathodes*, in *57th International Astronautical Congress* (2006), pp. C4–P. doi:10.2514/6.IAC-06-C4.P4.07
- [7] J. Polk, D. Goebel, R. Watkins, K. Jameson, L. Yoneshige, *Characterization of hollow cathode performance and thermal behavior*, in *42nd AIAA/ASME/SAE/ASEE Joint Propulsion Conference & Exhibit* (2006), p. 5150. doi:10.2514/6.2006-5150

- [8] C. Huo, F. Liang, A.b. Sun, Review on development of carbon nanotube field emission cathode for space propulsion systems. *High Voltage* **5**(4), 409–415 (2020). doi: [10.1049/hve.2019.0257](https://doi.org/10.1049/hve.2019.0257)
- [9] J. Zheng, J. Qin, K. Lu et al. Recent progress in chinese fusion research based on superconducting tokamak configuration. *The Innovation* **3**(4) (2022). doi: [10.1016/j.xinn.2022.100269](https://doi.org/10.1016/j.xinn.2022.100269)
- [10] D.M. Goebel, E. Chu, High-current lanthanum hexaboride hollow cathode for high-power hall thrusters. *Journal of Propulsion and Power* **30**(1), 35–40 (2014). doi: [10.2514/1.B34870](https://doi.org/10.2514/1.B34870)
- [11] D.M. Goebel, K.K. Jameson, R.R. Hofer, Hall thruster cathode flow impact on coupling voltage and cathode life. *Journal of Propulsion and Power* **28**(2), 355–363 (2012). doi: [10.2514/1.B34275](https://doi.org/10.2514/1.B34275)
- [12] J. Yanhui, Z. Tianping, Latest development of space-borne lab6 hollow cathode. *Chinese Journal of Vacuum Science and Technology* **36**(6), 690–698 (2016). doi: [10.13922/j.cnki.cjovst.2016.06.15](https://doi.org/10.13922/j.cnki.cjovst.2016.06.15)
- [13] D.M. Goebel, R.M. Watkins, K.K. Jameson, Lab6 hollow cathodes for ion and hall thrusters. *Journal of Propulsion and Power* **23**(3), 552–558 (2007). doi: [10.2514/1.25475](https://doi.org/10.2514/1.25475)
- [14] C. Drobny, J. Wulfkühler, K. Wätzig, M. Tajmar, Detailed work function measurements and development of a hollow cathode using the emitter material c12a7 electride. *SP2018–92*, Seville, Spain (2018)
- [15] J. Zheng, H. Liu, Y. Song et al., Integrated study on the comprehensive magnetic-field configuration performance in the 150 kw superconducting magnetoplasmadynamic thruster. *Scientific Reports* **11**(1), 20706 (2021). doi: [10.1038/s41598-021-00308-4](https://doi.org/10.1038/s41598-021-00308-4)
- [16] Z. Tian-Ping, T. Fu-Jun, T. Hua-Bing, Foreign technique status of hollow cathode for electric propulsion. *Aerospace Shanghai* (2008). doi: [10.19328/j.cnki.1006-1630.2008.01.009](https://doi.org/10.19328/j.cnki.1006-1630.2008.01.009)
- [17] L. Pengfei, F. Jinglian, H. Yong, Z. Man, T. Jiamin, Toughening mechanisms and interfacial bonding of w-zrc composites. *RARE METAL MATERIALS AND ENGINEERING* **48**(3), 751–757 (2019)
- [18] W. Yinhe, Y. Jiancan, C. Ran, G. Yinchun, Research on erosion resistance of rare earth tungsten electrode in electric propulsion. *RARE METAL MATERIALS AND ENGINEERING* **51**(10), 3892–3899 (2022). doi: [10.26935/d.cnki.gbju.2022.000326](https://doi.org/10.26935/d.cnki.gbju.2022.000326)
- [19] S. Wang, X. Zhang, N. Liu, et al., Recent Advances in Research and Development of Emissive Materials for Hollow Cathodes of Electric Propulsion Systems. *Chinese Journal of Vacuum Science and Technology* **43**(12), 993–1002 (2023). doi: [10.13922/j.cnki.cjvst.202306004](https://doi.org/10.13922/j.cnki.cjvst.202306004)
- [20] F. Peng, Z. Qin, T. Chen et al., Intrinsic emittance of thermionic cathode with work function variation. *Acta Electronica Sinica* **47**(3), 643–648 (2019). doi: [10.3969/j.issn.0372-2112.2019.03.018](https://doi.org/10.3969/j.issn.0372-2112.2019.03.018)
- [21] C. Spindt, I. Brodie, L. Humphrey et al., Physical properties of thin-film field emission cathodes with molybdenum cones. *Journal of Applied Physics* **47**(12), 5248–5263 (1976). doi: [10.1063/1.322600](https://doi.org/10.1063/1.322600)
- [22] D.A. Shiffler, M. Ruebush, D. Zagar et al., Emission uniformity and emittance of explosive field-emission cathodes. *IEEE Transactions on Plasma Science* **30**(4), 1592–1596 (2002). doi: [10.1109/TPS.2002.804172](https://doi.org/10.1109/TPS.2002.804172)
- [23] S.-K. Qi, X.-X. Wang, J.-R. Luo et al., A novel Y<sub>2</sub>O<sub>3</sub>-Gd<sub>2</sub>O<sub>3</sub>-HfO<sub>2</sub> impregnated w base direct-heated cathode in magnetron tube. *Acta Physica Sinica* **65**(5) (2016). doi: [10.7498/aps.65.057901](https://doi.org/10.7498/aps.65.057901)
- [24] K.L. Jensen, Y. Lau, N. Jordan, Emission nonuniformity due to profilimetry variation in thermionic cathodes. *Applied Physics Letters* **88**(16) (2006). doi: [10.1063/1.2197605](https://doi.org/10.1063/1.2197605)
- [25] F. Dong, H. Ye, W. Zhen, G. Jinyu, W. Hong, Preparation and electron emission properties of carbon fiber composited graphite cathodes. *Journal of Materials Engineering* **51**(8), 149–154 (2023). doi: [10.11868/j.issn.1001-4381.2023.000135](https://doi.org/10.11868/j.issn.1001-4381.2023.000135)
- [26] M.A. Chumak, E.O. Popov, S.V. Filippov, A.G. Kolosko, D.A. Kirilenko, N.A. Bert, E.V. Zhizhin, A.V. Koroleva, I.S. Yezhov, M.Y. Maximov, Reducing and tuning the work function of field emission nanocomposite cnt/nio cathodes by modifying the chemical composition of the oxide. *Nanoscale* **16**(21), 10398–10413 (2024). doi: [10.1039/D4NR00908H](https://doi.org/10.1039/D4NR00908H)
- [27] E. Wimmer, Computational materials design with first-principles quantum mechanics. *Science* **269**(5229), 1397–1398 (1995). doi: [10.1126/science.269.5229.139](https://doi.org/10.1126/science.269.5229.139)
- [28] M. Xia, P. Boulet, M.C. Record, Influence of biaxial and isotropic strain on the thermoelectric performance of pbsntese high-entropy alloy: A density-functional theory study. *Materials Today Physics* **49**, 101590 (2024). doi: [10.1016/j.mtphys.2024.101590](https://doi.org/10.1016/j.mtphys.2024.101590)
- [29] X.H. Fan, B. Xu, Y. Xu et al., Application of materials studio modeling in crystal structure. *Advanced Materials Research* **706**, 7–10 (2013). doi: [10.4028/www.scientific.net/AMR.706-708.7](https://doi.org/10.4028/www.scientific.net/AMR.706-708.7)
- [30] D. Jennison, P. Schultz, D. King et al., Bao/W(100) thermionic emitters and the effects of Sc, Y, La, and the density functional used in computations. *Surface Science* **549**(2), 115–120 (2004). doi: [10.1016/j.susc.2003.10.027](https://doi.org/10.1016/j.susc.2003.10.027)
- [31] A. Knizhnik, A. Safonov, I. Iskandarova et al., First-principles investigation of the wc/ hfo2 interface properties. *Journal of Applied Physics* **99**(8) (2006). doi: [10.1063/1.2189209](https://doi.org/10.1063/1.2189209)
- [32] Q. Zhang, F. Tang, Z. Zhao et al., Surface modification of tungsten oxide by oxygen vacancies for hydrogen adsorption. *Journal of Materials Science & Technology* **117**, 23–35 (2022). doi: [10.1016/j.jmst.2021.10.048](https://doi.org/10.1016/j.jmst.2021.10.048)
- [33] C. Wei, J. Fan, H. Gong, Tungsten adsorption on la2o3 (001) surfaces. *Materials Letters* **161**, 313–316 (2015). doi: [10.1016/j.matlet.2015.08.115](https://doi.org/10.1016/j.matlet.2015.08.115)
- [34] W. Peng, W. Yibai, L. Yong et al., Cathode erosion site distributions in an applied-field magnetoplasmadynamic thruster. *Plasma Science and Technology* **22**(9), 094008 (2020). doi: [10.1088/2058-6272/ab9172](https://doi.org/10.1088/2058-6272/ab9172)
- [35] M. Vilémová, K. Illková, F. Lukáč et al., Microstructure and phase stability of w-cr alloy prepared by spark plasma sintering. *Fusion Engineering and Design* **127**, 173–178 (2018). doi: [10.1016/j.fusengdes.2018.01.012](https://doi.org/10.1016/j.fusengdes.2018.01.012)
- [36] C. Wenge, Z. Hui, D. Bingjun, Advances in study on w-la2o3 electrode materials. *Ordnance Material Science and Engineering* **25**(4), 55 (2002). doi: [10.14024/j.cnki.1004-244x.2002.04.015](https://doi.org/10.14024/j.cnki.1004-244x.2002.04.015)
- [37] Z. Dong, Z. Ma, L. Yu et al., Achieving high strength and ductility in ods-w alloy by employing oxide@ w core-shell nanopowder as precursor. *Nature Communications* **12**(1), 5052 (2021). doi: [10.1038/s41467-021-25283-2](https://doi.org/10.1038/s41467-021-25283-2)
- [38] J. Xu, Z. Gu, X. Xi et al., Loss mechanism and lifetime estimation of ce-w cathode in high temperature thermionic emission electrostatic precipitation. *Journal of Electrostatics* **72**(4), 336–341 (2014). doi: [10.1016/j.elstat.2014.06.003](https://doi.org/10.1016/j.elstat.2014.06.003)
- [39] C. Cao, C. Wang, J. Ma, et al., Research on sintering techniques by hollow cathode discharge for tungsten and its alloy. *Hot Working Technology* **38**(10), 22–24, 28 (2009). doi: [10.14158/j.cnki.1001-3814.2009.10.038](https://doi.org/10.14158/j.cnki.1001-3814.2009.10.038)

- [40] A. Sengupta, *Destructive physical analysis of hollow cathodes from the deep space I flight spare ion engine 30,000 hr life test* (Pasadena, CA: Jet Propulsion Laboratory, National Aeronautics and Space, 2005)
- [41] A. Sengupta, J. Brophy, K. Goodfellow, Status of the Extended Life Test of the DS1 Flight Spare Ion Engine after 30,352 Hours of Operation, in *40th Joint Propulsion Conference, Fort Lauderdale, FL* (2004).doi: [10.2514/6.2003-4558](https://doi.org/10.2514/6.2003-4558)
- [42] J.T. Yim, G.C. Soulas, R. Shastry, M. Choi, J.A. Mackey, T.R. Sarver-Verhey, *Update of the NEXT ion thruster service life assessment with post-test correlation to the long duration test, in International Electric Propulsion Conference (IEPC) 2017* (2017), IEPC-2017-061
- [43] G.A. Csiky, Langmuir probe measurements in a discharge from a hollow cathode. *Journal of Spacecraft and Rockets* **7**(4), 474–475 (1970). doi: [10.2514/3.29966](https://doi.org/10.2514/3.29966)
- [44] W.G. Seo, J.W. Kuk, H. Kim et al., Micro/Nano Scale Emission Tip Fabrication for Field Emission Electric Propulsion, in *2023 IEEE 22nd International Conference on Micro and Nanotechnology for Power Generation and Energy Conversion Applications (PowerMEMS)* (IEEE, 2023), pp. 252–255. doi: [10.1109/PowerMEMS59329.2023.10417347](https://doi.org/10.1109/PowerMEMS59329.2023.10417347)
- [45] C.M. Marrese, *A review of field emission cathode technologies for electric propulsion systems and instruments, in 2000 IEEE Aerospace Conference. Proceedings (Cat. No. 00TH8484)*, vol. 4 (IEEE, 2000), pp.85–98. doi: [10.1109/AERO.2000.878369](https://doi.org/10.1109/AERO.2000.878369)
- [46] L. Xin, W. Xuan, T. Hai-bin, Z. Zhe, K. Xiao-lu, Beam characteristics of het-80 hall thruster with 700 watts. *Journal of Propulsion Technology* **39**(6), 1426. doi:[10.13675/j.cnki.tjjs.2018.06.028](https://doi.org/10.13675/j.cnki.tjjs.2018.06.028)